

# POSSIBLE SIGNATURES OF MAGNETOSPHERIC ACCRETION ONTO YOUNG GIANT PLANETS

R.V.E. LOVELACE<sup>1</sup>, K.R. COVEY<sup>2,3,4</sup>, AND J.P. LLOYD<sup>2</sup>  
*Draft version October 30, 2018*

## ABSTRACT

Magnetospheric accretion is an important process for a wide range of astrophysical systems, and may play a role in the formation of gas giant planets. Extending the formalism describing stellar magnetospheric accretion into the planetary regime, we demonstrate that magnetospheric processes may govern accretion onto young gas giants in the isolation phase of their development. Planets in the isolation phase have cleared out large gaps in their surrounding circumstellar disks, and settled into a quasi-static equilibrium with radii only modestly larger than their final sizes (i.e.,  $r \sim 1.4r_{\text{final}}$ ). Magnetospheric accretion is less likely to play a role in a young gas giant's main accretion phase, when the planet's envelope is predicted to be much larger than the planet's Alfvén radius. For a fiducial  $1 M_J$  gas giant planet with a remnant isolation phase accretion rate of  $\dot{M}_\odot = 10^{-10} M_\odot \text{yr}^{-1} = 10^{-7} M_J \text{yr}^{-1}$ , the disk accretion will be truncated at  $\sim 2.7r_J$  (with  $r_J$  is Jupiter's radius) and drive the planet to rotate with a period of  $\sim 7$  hours. Thermal emission from planetary magnetospheric accretion will be difficult to observe; the most promising observational signatures may be non-thermal, such as gyrosynchrotron radiation that is clearly modulated at a period much shorter than the rotation period of the host star.

*Subject headings:* accretion, accretion disks — planets — etc

## 1. INTRODUCTION

Magnetically controlled accretion (e.g. Ghosh & Lamb 1979) governs mass accretion onto objects ranging from white dwarfs and neutron stars (Warner 2004) to super-massive black holes (Koide et al. 1999). Magnetospheric accretion models (Königl 1991) explain many of the observational characteristics of young stars, such as the presence and magnitude of UV excesses from accretion shocks (Calvet & Gullbring 1998; Herczeg & Hillenbrand 2008) and the kinematic structure and rotational modulation of spectral line profiles arising from accretion funnel flows (e.g. Bouvier et al. 2003, Kurosawa et al. 2006).

Hydrodynamical simulations of mass accretion onto young giant planets have been performed (e.g., Papaloizou & Nelson 2005; Hubickyj, Bodenheimer, & Lissauer 2005; Ayliffe & Bate 2009), but these analyses have not formally considered the influence of the planet's magnetic field. Young gas giants likely possess strong dynamos, driven by rapid rotation and significant convective motions in their interiors (Sánchez-Lavega 2004). The appreciable large-scale magnetic fields produced by these dynamos could channel subsequent accretion onto the giant planet, potentially producing observational signatures analogous to those observed in young stars.

Earlier, Quillen and Trilling (1998) and Fendt (2003) discussed magneto-centrifugally driven outflows from the circumplanetary disks. Fendt considered planetary accretion rates  $\sim 10^{-6} M_\odot \text{yr}^{-1} = 10^{-3} M_J \text{yr}^{-1}$ . Our analytic calculations, combined with recent estimates of proto-planetary radii, imply that the planet's magnetic field is likely to be buried for such a high accretion rate. That is, the planet's physical radius will be larger than the magnetic standoff or Alfvén radius. The focus of the

present work is on the conditions with much slower accretion ( $\sim 10^{-10} M_\odot \text{yr}^{-1}$ ), where the planet's magnetic field is not buried so that it may influence the planet's accretion. This value of the accretion rate agrees with that considered by Quillen and Trilling (1998). The present work is concerned with the possible time-dependence of the rotating planet's emission due to its non-symmetric magnetosphere rather than its outflows.

Our interest in this problem was motivated by recent observations of a young stellar object, IC1396A-47, whose mid-IR light curve reveals periodicities on two very different timescales (Morales-Calderón et al. 2009). The long-period variability ( $P_{\text{rot}} \approx 9$  d;  $\delta[3.6] \sim 0.2$  mag.) is likely due to the rotation of a hot spot on the surface of the star, but the origin of the short-period component ( $P_{\text{rot}} \approx 3.5$  hr.;  $\delta[4.5] \sim 0.04$  mag.) is less clear. Morales-Calderón et al. conclude that  $\delta$  Scuti pulsations are the most likely explanation for the short-period variability, but the timescale is also within the range of rotation periods expected for young planets.

In this letter, we explore potential observational signatures of magnetospherically accreting young planets. In Section 2 we derive analytic expressions that describe magnetospheric accretion in the planetary regime. With few observational constraints on the physical properties of young gas giants, we investigate in Section 3 predictions of our magnetospheric accretion model over the area of parameter space potentially inhabited by proto-gas giants. We explore potential observational signatures of this process in Section 4, and summarize our conclusions in Section 5.

## 2. MAGNETOSPHERIC ACCRETION TO GIANT PLANETS

<sup>1</sup> Departments of Astronomy and Applied and Engineering Physics, Cornell University, Ithaca, NY 14853-6801; RVL1@cornell.edu

<sup>2</sup> Department of Astronomy, Cornell University, Ithaca, NY 14853-6801; kcovey@astro.cornell.edu; jpl@astro.cornell.edu

<sup>3</sup> Hubble Fellow

<sup>4</sup> Visiting Scholar, Department of Astronomy, Boston University, Boston MA 02215

We consider the early stage ( $\lesssim 10$  Myr) of a giant planet of mass  $M_p$  (of the order of Jupiter’s mass) orbiting a young star surrounded by an accretion disk. Giant planets are thought to form at  $R_p \sim 10 - 25$  AU from the star and then undergo Type II inward migration at roughly the viscous accretion speed of the disk (Papaloizou et al. 2007).

Critical parameters for magnetospheric accretion by a giant planet are the planet’s characteristic radius, where an accretion shock may form, and its accretion rate. These parameters are strongly time-dependent during the planet’s formation. Planets with high mass accretion rates ( $\sim 10^{-8} M_\odot \text{yr}^{-1}$ ) are predicted to have radii much larger than Jupiter’s radius (denoted  $r_J$ ; Hubickyj, Bodenheimer, & Lissauer 2005; Helled & Schubert 2008; Ayliffe & Bate 2009). The planet quickly cools once the mass accretion slows significantly, however, with models predicting a rapid collapse to much smaller radii ( $\sim r_J$ ; Lissauer et al. 2009).

In the core accretion model, a gas giant grows as its rocky core accretes material within its Hill radius,  $r_H = R_p [M_p / (3M_*)]^{1/3}$ , where  $M_*$  is the star’s mass, and  $M_p$  is the planet’s mass (e.g., Hubickyj, Bodenheimer, & Lissauer 2005). The planet’s Hill radius expands as its mass increases, enabling the planet to accrete mass from a larger portion of the circumstellar disk. The planet’s mass accretion rate thus increases until its Hill radius exceeds the scale height of the circumstellar disk. This isolates the planet within a gap in the circumstellar disk, at which point Type II migration begins (e.g., Papaloizou et al. 2007). This is sketched in Figure 1.

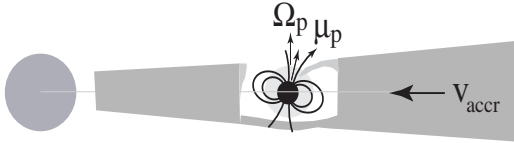


FIG. 1.— Envisioned geometry of a giant, gap-forming planet in the accretion disk of a young star.

The gap the planet opens in the circumstellar disk does not stop accretion to the planet (e.g., Alexander & Armitage 2009). Tidal streams flow across the gap in the disk, sustaining the mass accretion rate onto the planet ( $\dot{M}_p$ ) and the star ( $\dot{M}_*$ ) at some fraction of the disk accretion rate expected in the absence of a planet ( $\dot{M}_d$ ; Lubow et al 1999, D’Angelo et al. 2002).

When the planet’s radius  $r_p \ll r_H$ , matter accreting to the planet will in-spiral in a Keplerian disk from roughly  $r_H/3$  to the planet’s surface (Ayliffe & Bate 2009). The nominal *accretion luminosity* of this circumplanetary disk is

$$L_{pd} = \frac{GM_p \dot{M}_p}{r_p} \approx 10^{29} \frac{1}{\mathcal{R}_p} \frac{M_p}{M_J} \frac{\dot{M}_p}{\dot{M}_0} \frac{\text{erg}}{\text{s}}. \quad (1)$$

Here,  $M_J$  is Jupiter’s mass ( $1.9 \times 10^{30}$  g),  $r_J$  is Jupiter’s radius ( $7.14 \times 10^9$  cm) and  $\mathcal{R}_p \equiv r_p/r_J$ . We assume  $\mathcal{R}_p \approx 1.3$ , as found by Fortney, Baraffe, & Militzer (2009) at  $t = 10^7$  yr.

## 2.1. Magnetic disk locking of planets

If the planet is unmagnetized and accretes  $\gtrsim 10\%$  of its mass from a circumplanetary disk, it will spin-up to a break-up angular velocity  $\Omega_{\text{max}} = (GM_p/r_p^3)^{1/2}$ . This break-up velocity corresponds to a minimum rotation period of  $T_{\text{min}} \approx 3(M_J/M_p)^{1/2} \mathcal{R}_p^{3/2} \text{hr} \approx 4.4 \text{hr}$  for  $M_p = M_J$  and  $\mathcal{R}_p = 1.3$ . Accretion to a planet rotating at break-up continues via mechanisms describing of disk accretion to a rapidly rotating unmagnetized star (Bisnovatyi-Kogan 1993).

Magnetic processes may influence accretion onto the planet. The planet’s rapid rotation and convective interior suggest strong dynamo activity that could produce appreciable large-scale, dipole magnetic fields (Sánchez-Lavega 2004). As a reference value we adopt a magnetic moment for young gas giants of 10 times the magnetic moment of Jupiter ( $\mu_J$ ; Sánchez-Lavega 2004), or a surface magnetic field of about 85G at the magnetic pole for a Jupiter size planet. This magnetic field may be strong enough to truncate the circumplanetary disk at the Alfvén radius, where the kinetic energy density of the disk plasma ( $\rho v_K^2/2$ , with  $v_K = \sqrt{GM_p/r_p}$ , the disk’s Keplerian velocity) is equal to the energy density of the magnetic field ( $\mathbf{B}^2/8\pi$ ; Davidson & Ostriker 1973; Elsner & Lamb 1977; Long, Romanova, & Lovelace 2005). The Alfvén radius of an accreting, *non-rotating planet* ( $r_{A0}$ ) can be expressed as

$$r_{A0} \approx \left( \frac{\mu_p^2}{\dot{M}_p \sqrt{GM_p}} \right)^{2/7} \approx 10^{10} \left( \frac{\mu_p}{10\mu_J} \right)^{4/7} \left( \frac{\dot{M}_0}{\dot{M}_p} \right)^{2/7} \left( \frac{M_J}{M_p} \right)^{1/7} \text{ cm} \quad (2)$$

where  $\mu_J$  is the magnetic moment of Jupiter and  $\mu_p$  is the magnetic moment of the young gas giant.

A rotating giant planet’s effective Alfvén radius is actually somewhat larger than that implied by the first order calculation in Equation 2. This effect can be understood by noting that the Alfvén radius is the distance where the kinetic energy of the disk plasma in the *reference frame rotating with the planet* is equal to the magnetic energy density. This implies that the effective Alfvén radius will be larger for rapidly rotating planets, as the planet’s rotation will reduce the velocity contrast between the planet’s magnetic field and the Keplerian motion in the circumplanetary disk. The effective Alfvén radius for a rotating planet can be calculated as  $r_A = r_{A0} [1 - \Omega_p r_A / v_K(r_A)]^{-4/7}$  or  $\eta_A^{-7/2} = (1 - g \omega_p \eta_A^{3/2})^2$ , where  $\eta_A \equiv r_A/r_{A0}$ ,  $\omega_p \equiv \Omega_p/\Omega_{\text{max}}$  with  $0 \leq \omega_p \leq 1$ , and  $g \equiv \Omega_{\text{max}}(GM_p/r_{A0}^3)^{-1/2}$ .

The relation between  $\eta_A$  and  $\omega_p$  can be rewritten as

$$\omega_p = (\eta_A^{-3/2} \pm \eta_A^{-13/4}) g^{-1}. \quad (3)$$

The solid lines in Figure 2 show the relationship between  $\omega_p$  and  $\eta_A$  for the reference values of equation (2), which give  $g = 0.636$ . We do not consider tidal locking of the planet’s rotation, which is estimated to take longer than 10 Myr for  $R_p > 0.1$  AU.

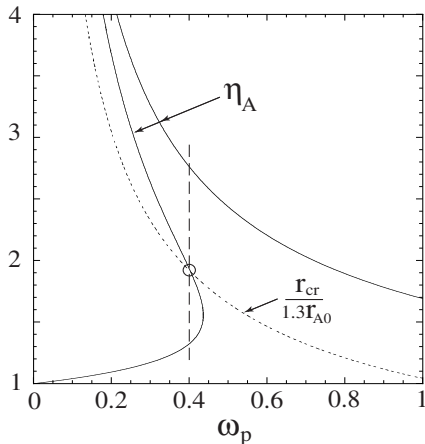


FIG. 2.— The solid curves show the relation between  $\eta_A = r_A(\omega_p)/r_{A0}$  and  $\omega_p = \Omega_p/\Omega_{\max}$  from equation (3). The dotted curve shows  $r_{\text{cr}}(\omega_p)/(1.3r_{A0})$ . The intersection of the dotted and solid curve corresponds to disk locking as discussed in the text.

While the planet's rotation influences where the circumplanetary disk is truncated, transfer of angular momentum between the planet and circumplanetary disk via magnetic interactions also influences the planet's rotation rate. This feedback mechanism drives towards an equilibrium state where there is no net angular momentum flow between the planet and the inner edge of the circumplanetary disk (Ghosh & Lamb 1979). Simulations of magnetospheric accretion have identified that stars in this 'disk-locked' state rotate more slowly than break-up ( $\Omega_p < \Omega_{\max}$ ), such that the Alfvén radius slightly exceeds the 'co-rotation radius' ( $r_{\text{cr}}$ ), where the angular velocity of Keplerian motion in the disk equals the star's angular velocity (i.e.,  $r_{\text{cr}} \equiv (GM_p/\Omega_p^2)^{1/3} \approx 1.6 \times 10^{10} (M_p/M_J)^{1/3} (\Omega_J/\Omega_p)^{2/3} \text{cm} \approx 1.3r_A$ ; Long et al. 2005). This is equivalent to the condition that  $r_{\text{cr}}(\omega_p)/(1.3r_{A0}) = \eta_A(\omega_p)$ . Figure 2 shows both  $r_{\text{cr}}(\omega_p)/(1.3r_{A0})$  (dotted curve) and  $\eta_A(\omega_p)$  (solid curves from equation 3). Their intersection point (indicated by the circle) corresponds to disk-locking. Along the vertical dashed line *above* the circle, where the line intersects at  $\eta_A > r_{\text{cr}}/(1.3r_{A0})$ , the planet will *spin-down*, whereas below the circle where the line intersects at  $\eta_A < r_{\text{cr}}/(1.3r_{A0})$ , the planet will *spin-up* (see Lovelace, Romanova, & Bisnovaty-Kogan 1999).

## 2.2. Magnetospheric accretion from the circumplanetary disk

The matter inflow from the inner edge of the circumplanetary disk at  $r_A$  to the planet's surface at  $r_p$  occurs in narrow "funnel streams" which follow the planet's magnetic field as proposed by Ghosh and Lamb (1979) and observed and analyzed in three-dimensional magnetohydrodynamic (MHD) simulations by Romanova et al. (2002, 2004). If the planet's magnetic dipole moment  $\mu_p$  is not greatly misaligned with the planet's rotation axis  $\Omega_p$  (assumed perpendicular to the disc around the star), then the funnel streams will impact the planet's surface close to the magnetic poles roughly perpendicular to the surface. The funnel streams are approximately stationary in a reference frame rotating with the planet (Romanova et al. 2004). Thus, the flow speed along the funnel stream  $u_f(r)$  is obtained from Bernoulli's law in a reference frame

rotating with angular rate  $\Omega_p$ . This gives

$$\frac{u_f^2}{2} + \Phi(r_p) = \frac{1}{2} [v_K(r_A) - \Omega_p r_A]^2 + \Phi(r_A), \quad (4)$$

where  $v_K(r_A)$  is the azimuthal velocity of the disk matter at  $r_A$  and  $\Phi(r) = -GM_p/r - \Omega_p^2 r^2/2$  is the effective potential.

The impact of a funnel stream on the planet's surface will create a strong shock wave covering a small fraction of the planet's surface - a "hot-spot" - where the power in the stream is thermalized and radiated away. Just outside the shock wave we have  $\dot{M}_p = 2\pi r_{fp}^2 \rho_{fp} u_{fp}$ , where  $r_{fp}$  is the radius of the funnel stream at the planet's surface and  $\rho_{fp}$  is the density before the shock. Translating into the planetary regime the results of the 3D MHD simulations of stellar mass accretion described above implies that  $r_{fp} = (0.1 - 0.2)r_p$  (Romanova et al. 2004). The power dissipated behind the shock is assumed to be radiated as black-body radiation so that the effective temperature of the hot-spot is simply

$$T_{\text{eff}} = \left( \frac{\rho_{fp} u_{fp}^3}{2\sigma} \right)^{1/4}, \quad (5)$$

where  $\sigma = 5.67 \times 10^{-5} \text{ cgs}$  is the Stefan-Boltzmann constant.

Figure 3 shows an example of a funnel flow obtained from three dimensional magnetohydrodynamic simulations by Romanova, Kulakrni, & Lovelace (2008).

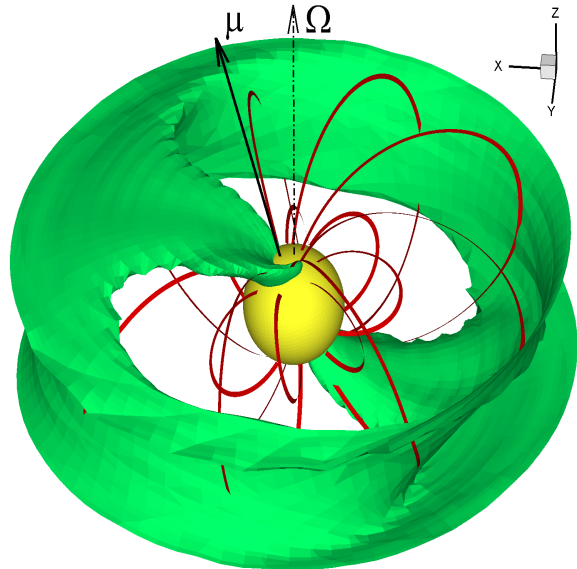


FIG. 3.— Funnel flow onto a rotating magnetized object from 3D MHD simulations by Romanova, Kulkarni, and Lovelace (2008). The red lines are magnetic field lines,  $\mu$  is the magnetic moment,  $\Omega$  is the angular velocity vector. The green color labels an isodensity surface. Inside of the green surface the density is higher.

## 2.3. Parameters of Accreting Magnetized Giant Planets

The previous subsections give a general description of accreting, rotating magnetized giant planets. The focus of the present work is on the conditions where the magnetic field of the rotating planet influences the planet's accretion. Evidently, the planet's magnetic field can have a significant influence on its accretion only under conditions where the planet's Alfvén radius exceeds its physical radius. Otherwise, the magnetic field will be too weak to

channel the accreting material into funnel streams. As is clear by inspection of Equation 2, the most time-variable parameter governing a planet's Alfvén radius is its accretion rate, which is likely to change more rapidly than its mass or magnetic moment. To explore the area of parameter space in which magnetic effects will be important, we plot in Figure 4 the Alfvén radius and possible planet radii (discussed below) as a function of the planet's accretion rate  $\dot{M}_p$  measured in units of  $\dot{M}_0 \equiv 10^{-10} M_\odot \text{yr}^{-1}$ . For this plot we assume  $M_p = M_J$  and  $\mu_p = 10\mu_J$ .

Theoretical models of gas giant protoplanets have been developed by Papaloizou and Nelson (2005). They consider two models, an early stage of planet formation - termed type A - where the planet is an extended structure going out to its Hill sphere, and a later stage - termed type B - where the protoplanet is much more compact with a free surface which accretes from a circumplanetary disk. Both models start from solid cores of 5 or  $15M_\oplus$ . The type A models are found to have long mass accretion time-scales for  $M_p \lesssim 30M_\oplus$  and they may undergo rapid type I inward migration unless this migration is suppressed (e.g., Rafikov 2002; Li et al. 2009). In the type B models the planet's radius approaches  $\sim 2 \times 10^{10}$  cm and is relatively independent of the accretion rate  $\dot{M}_p$  which is determined by star's accretion disk. The planet undergoes slower type II migration. In Figure 4 the horizontal dashed lines indicate the planet's radii for type A and B models.

Numerical simulations of planet formation also give information on the physical radii of young gas giants as functions of mass and time. Hubickyj et al. (2005) and Ayliffe & Bate (2009) find that a young ( $t < 2$  Myrs) proto-Jupiter ( $M_p = M_J$ ) has a typical mass accretion rate of  $\sim 3 \times 10^{-8} M_\odot/\text{yr}$ , and a radius of  $\sim 100R_J$  which is of the order of the radii of the type A models of Papaloizou and Nelson (2005). It is not clear why the simulations do not give the Papaloizou and Nelson type B solutions. Figure 4 includes the line marked C for an older ( $t > 10$  Myr) non-accreting Jupiter-mass planet predicted by Fortney et al. (2009) to have a radius  $\sim 1.3r_J$ .

From Figure 4, it is apparent that planets with accretion rates  $\gtrsim \dot{M}_0 \equiv 10^{-10} M_\odot/\text{yr}$  have physical radii larger than their Alfvén radii so that the planet's accretion will not be affected by its magnetic field. Magnetospheric accretion may, however, be important once a gas giant ends its main accretion phase (type A models of Papaloizou & Nelson, 2005), having entered a type B model with an extended circumplanetary disk. For the accretion rates considered by Fendt (2003) ( $\sim 10^{-6} M_\odot \text{yr}^{-1}$ ), we expect that the planet's radius is larger than the Alfvén radius.

In the following we consider a fiducial model with  $\dot{M}_p = \dot{M}_0 \equiv 10^{-10} M_\odot \text{yr}^{-1} \approx 10^{-7} M_J \text{yr}^{-1}$ . In the equilibrium disk-locked state, the planet rotates with  $\omega_p \approx 0.4$  and truncates its circumplanetary disk at  $r_A = 1.9r_{A0}$ . For our fiducial gas giant planet, this corresponds to a rotation period of  $2\pi/\Omega_p \approx 7.4$  hr, somewhat less than Jupiter's rotation period of 9.8 hr. For our adopted reference values this gives a flow speed at the planet's surface  $u_f(r_p) = u_{fp} \approx 21 \text{ km s}^{-1}$ .

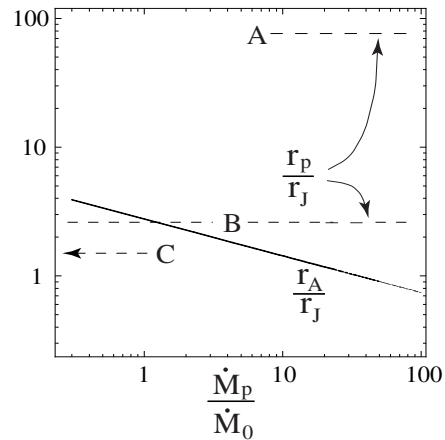


FIG. 4.— The solid curve gives the effective Alfvén radius  $r_A \approx 1.9r_{A0}$  in units of Jupiter's radius  $r_J$  from Eq. 2 assuming the planet's magnetic moment is  $10\mu_J$ . The factor of 1.9 is discussed in the text. Here,  $\dot{M}_0 = 10^{-10} M_\odot/\text{yr} \approx 10^{-7} M_J/\text{yr}$ . The dashed curve shows a sketch of the planet's radius  $r_p$  in units of  $r_J$  estimated from the work of Hubickyj et al. (2005) for times  $t \lesssim 2\text{Myr}$  and from the work of Fortney et al. (2009) for  $t \gtrsim 10\text{Myr}$ .

### 3. OBSERVATIONAL SIGNATURES OF ACCRETING GIANT PLANETS

We now use the analytic framework described above to consider potential observational signatures of planetary magnetospheric accretion. In turn, we explore the basic thermal signature of this process, the potential to spatially or temporally resolve this thermal signature, and finally non-thermal observables.

**Thermal Signatures:** The equations in section 2 allow us to describe the basic thermal properties of the accretion shock and circumplanetary disk associated with a giant planet undergoing magnetospheric accretion. The accretion shock is likely the warmer of the two components, and thus more amenable to observations at the shorter wavelengths accessible to ground based observatories. For our reference values and  $r_{fp} = 0.2r_p$  we find the accretion shock's  $T_{\text{eff}} \approx 2100$  K, whereas for  $r_{fp} = 0.1r_p$ ,  $T_{\text{eff}} = 3000$  K. This temperature is somewhat less than the temperature of a typical T Tauri star photosphere ( $T_{\text{eff}} \sim 4000\text{K}$ ; Johns-Krull & Gafford 2002), providing some leverage for decomposing these two components of a star's spectral energy distribution.

The true challenge of detecting the thermal signature of a planetary accretion shock becomes apparent, however, when one considers the overall luminosity of the shock in contrast to that of the stellar photosphere. The power dissipated in one hemisphere's accretion hot-spot is  $\dot{M}_p u_{fp}^2/4$  which is about  $0.063L_{pd}$  for our fiducial model. As  $L_{pd}$  is on the order of  $10^{29} \text{ erg/s}$ , this indicates an observable accretion luminosity of  $\approx 10^{27-28} \text{ erg/s}$ . T Tauri stars, however, have typical photospheric luminosities of  $L_* \approx 10^{33} \text{ erg s}^{-1}$ , and young giant planets are thought to have luminosities of  $10^{27-30} \text{ ergs}^{-1}$  (Hubickyj et al. 2005; Marley et al. 2007). Detecting the thermal signature of a planetary accretion shock will therefore require disentangling three blackbody spectra to identify a component that contributes just one of every million photons detected from a given young stellar object.

The other thermal signature of planetary magnetospheric accretion will arise from the circumplanetary disk. The effective temperature of the disk, which we assume to be optically thick, is  $T_{\text{effp}} = [3GM_p\dot{M}_p/(16\pi\sigma)]^{1/4} \approx 1200(r_J/r)^{3/4}(M_p/M_J)^{1/4}(M_p/M_\odot)^{1/4}$  K, where  $r$  is the distance from the planet's center. If the circumplanetary disk is truncated at  $r_A \sim 2r_{A0} \sim 2.7r_J$ , the inner edge of the disk is predicted to have a temperature of  $\sim 1200$  K, much higher than the local temperature of the star's disk for  $R_p \gg 0.25$  AU. The ratio of the luminosity of the planet's disk ( $GM_p\dot{M}_p/2r_p$ ) to the luminosity of the annular region of the star's disk of width  $2r_H$  (in the absence of the planet) is  $(M_p/3M_*)(\dot{M}_p/\dot{M}_*)(R_p/r_p)(R_p/r_H)$ . For a giant planet of Jupiter's mass and semimajor radius and  $M_* = M_\odot$ , this ratio is  $\sim 50(\dot{M}_p/\dot{M}_*)$ . While the circumplanetary disk may be more luminous than the surrounding material in the circumstellar disk, the emission from the circumplanetary disk may be difficult to disentangle from the young planet itself, which could well have a similar temperature and luminosity ( $L \sim 10^{-6}$  to  $10^{-3}L_\odot$ ,  $T_{\text{eff}} \sim 500$  to  $2000$  K; Marley et al. 2007). Spatially resolving a truncated circumplanetary disk would provide a clear observable signal, but resolving spatial scales of  $r_J$  in Taurus ( $d \sim 140$  pc; Loinard et al. 2007) requires high contrast observations on angular scales of  $10$ – $6''$ , well beyond current observational capabilities.

The hot-spots can give periodic variations in the observed radiation depending on the angle  $\Theta$  between the planet's magnetic moment  $\mu$  and its rotation axis  $\Omega_p$  and the angle  $\iota$  between the line-of-sight to the object and  $\Omega_p$  as analyzed by Romanova et al. (2004). This work assumes that the planet's rotation axis is the same as the rotation axes of the disk and the star. Thus we do not consider close-in giant planets where the planet's orbital angular momentum is in some cases observed to be misaligned with the star's angular momentum (e.g., Triaud et al. 2010). For  $\Theta = 0$  the planet is axisymmetric and there are no variations in the luminosity for any value of  $\iota$ . For  $\Theta \neq 0$  and  $\iota = 0$  the disk is face-on and there are no luminosity variations. For  $\Theta \neq 0$  and  $\iota$  larger than a critical value (possibly  $\sim 45^\circ$ ) dependent on the geometry of the gap in the disk the radiation from the hot spot will be obscured by the disk. Note that the misalignment or tilt angle of Jupiter's magnetic field is  $\Theta \approx 10^\circ$ .

To estimate of the magnitude of the fluctuations from a rotating giant planet we assume the host star to be a typical K7/M0 Classical T Tauri Star, and for specificity adopt the physical parameters measured for AA Tau:  $R_* = 1.67R_\odot$ ,  $T_{\text{eff}} = 4000$  K, and  $P_{\text{rot}} = 8$  days (Johns-Krull & Gafford 2002). Thus the star's photospheric luminosity is  $L_* \approx 2.5 \times 10^{33}$  erg s $^{-1}$ . To get an upper limit on the detectability of accretion onto a giant planet, we first assume 100% rotational modulation of the emission from the planet's 'hot spot'. For one hemisphere of the planet this is  $L_{hs+} \lesssim GM_p\dot{M}_p/(4r_p)$ , where  $M_p$ ,  $\dot{M}_p$ , and  $r_p$  are the planet's mass, accretion rate, and radius. The rotation period of the planet (3 – 10 hr) is not affected by the tidal interactions in 10 Myr for major radii  $> 0.1$  AU. We neglect the radiation from the star's accretion disk and accretion shock and the planet's disk. The fractional

variation in the flux due to the rotating planet is

$$\frac{L_{hs+}}{L_*} \lesssim 10^{-5} \left( \frac{M_p}{M_J} \right) \left( \frac{\dot{M}_p}{10^{-10} M_\odot \text{yr}^{-1}} \right) \left( \frac{r_J}{r_p} \right), \quad (6)$$

such that detecting this effect will require exquisitely precise, stable photometry.

**Non-Thermal Signatures:** For  $r_A > r_p$ , note that an accreting magnetized planet may produce oppositely directed conical winds and jets along its rotation axis  $\Omega_p$ . Analogous winds and jets are common features of young accreting magnetized stars (see review by Ray et al. (2007), and they have been studied in 2D and 3D magnetohydrodynamic simulations (e.g. Romanova et al. 2009). In agreement with estimates by Quillen and Trilling (1998) and Fendt (2003), we expect the mass outflow rate to be about  $0.1\dot{M}_p$  and the outflow velocity to be  $\sim v_K(r_p)$  which is about 42 km/s for a Jupiter mass planet and significantly larger than the escape speed from the star. It is also possible that the giant planet has magnetic reconnection flares analogous to those observed in young stars (e.g., Getman et al. 2008). However, the magnetic field strength of the planet is down by more than a factor of 10 from that of the star and the emission volume ( $V_e \propto R_p^3$ ) is down by a factor of  $10^3$  so that the flare energy ( $\propto B^2 V_e$ ) is down by more than a factor of  $10^5$  compared with that of the star. On the other hand high energy electrons produced in a flare are expected to propagate both outward and downward along the planet's field lines. The electrons reaching the planet's magnetic poles can give rise to gyrosynchrotron radiation in the radio band ( $\sim$ GHz). This type of circularly polarized radiation has been observed from T Tau S (Skinner & Brown 1994) and from embedded young class I objects (Feigelson, Carkner, & Wilking 1998; Choi et al. 2009). The radiation is thought to be analogous to that from RS CVn binary systems (e.g., Morris, Mutel, & Su 1990). Because this radiation (unlike the X-ray) comes from near the planet's surface with the emission  $\propto B^2$ , it may be modulated by the planet's rotation depending of course on  $\Theta$  and  $\iota$ .

#### 4. CONCLUSIONS

In this paper, we provide a first extension of the formalism describing stellar magnetospheric accretion into the planetary regime. In doing so, we demonstrate that:

1. Magnetospheric processes may govern accretion onto young gas giants in the isolation phase of their development. Magnetospheric accretion is less important for younger gas giants in their main accretion phase: thermal energy from accretion inflates their envelopes to sizes much larger than their magnetic Alfvén radius.
2. For a fiducial  $1 M_J$  gas giant planet with a remnant isolation phase accretion rate of  $\dot{M}_\odot = 10^{-10} M_\odot$ , magnetospheric accretion will truncate the circumplanetary disk at  $\sim 2$  Alfvén radii (corresponding to  $\sim 1.5$  planetary radii and  $\sim 3$  Jupiter radii), and drive the planet to rotate with a period of  $\sim 7$  hours.
3. Thermal emission from planetary magnetospheric accretion will be difficult to observe due to the stringent flux contrast and/or spatial resolution required for such measurements. The most promising observational signatures may be non-thermal, such as gyrosynchrotron radiation



that is clearly modulated at a period much shorter than the rotation period of the host star.

#### ACKNOWLEDGEMENTS

We thank M.M. Romanova, P.D. Nicholson, Sally Dodson–Robinson, M.S. Tiscareno, M.M. Hedman, and E.D. Feigelson for valuable comments and discussions. RVEL was supported in part by NASA grant

NNX08AH25G and by NSF grants AST-0607135 and AST-0807129. Support for this work was provided by NASA through Hubble Fellowship grant HST-HF-51253.01-A awarded by the Space Telescope Science Institute, which is operated by the Association of Universities for Research in Astronomy, Inc., for NASA, under contract NAS 5-26555.

#### REFERENCES

- Alexander, R.D., & Armitage, P.J. 2009, *ApJ*, 704, 989  
 Ayliffe, B.A., & Bate, M.R. 2009, *MNRAS*, 393, 49  
 Bisnovatyi-Kogan, G.S. 1993, *A&A*, 274, 796  
 Bouvier, J., et al. 2003, *A&A*, 409, 169  
 Calvet, N., & Gullbring, E. 1998, *ApJ*, 509, 802  
 Choi, M., Tatematsu, K., Hamaguchi, K., & Lee, J.-E. 2009, *ApJ*, 690, 1901  
 Davidson, K., & Ostriker, J.P. 1973, *ApJ*, 179, 585  
 Elsner, R.F., & Lamb, F.K. 1977, *ApJ*, 215, 897  
 Feigelson, E.D., Carkener, L., & Wilking, B.A. 1998, *ApJ*, 494, L215  
 Fendt, C. 2003, *A&A*, 411, 623  
 Fortney, J.J., Baraffe, I., & Militzer, B. 2009, *arXiv:0911.3154v1*  
 Getman, K.V., Feigelson, E.D., Micela, G., Jardine, M.M., Gregory, S.G., & Garmire, G.P. 2008, *ApJ*, 688, 437  
 Ghosh, P., & Lamb, F.K. 1979, *ApJ*, 234, 296  
 Helled, R., & Schubert, G. 2008, *Icarus*, 198, 156  
 Herczeg, G. J., & Hillenbrand, L. A. 2008, *ApJ*, 681, 594  
 Hubickyj, O., Bodenheimer, P., & Lissauer, J. J. 2005, *Icarus*, 179, 415  
 Johns-Krull, C. M., & Gafford, A. D. 2002, *ApJ*, 573, 685  
 Koide, S., Shibata, K., & Kudoh, T. 1999, *ApJ*, 522, 727  
 Königl, A. 1991, *ApJ*, 370, L39  
 Kurosawa, R., Harries, T. J., & Symington, N. H. 2006, *MNRAS*, 370, 580  
 Li, H., Lubow, S.H., Li, S., & Lin, D.N.C. 2009, *ApJ*, 690, L52  
 Lissauer, J. J., Hubickyj, O., D’Angelo, G., & Bodenheimer, P. 2009, *Icarus*, 199, 338  
 Loinard, L., Torres, R. M., Mioduszewski, A. J., Rodríguez, L. F., González-Lópezlira, R. A., Lachaume, R., Vázquez, V., & González, E. 2007, *ApJ*, 671, 546  
 Long, M., Romanova, M.M., & Lovelace, R.V.E. 2005, *ApJ*, 634, 1214  
 Lovelace, R.V.E., Romanova, M.M., & Bisnovatyi-Kogan, G.S. 1999, *ApJ*, 512, 368  
 Marley, M. S., Fortney, J. J., Hubickyj, O., Bodenheimer, P., & Lissauer, J. J. 2007, *ApJ*, 655, 541  
 Morales-Calderón, M., Stauffer, J.R., Rebull, L., Whitney, B.A., Barrado y Navascués, D., Ardila, D.r., Song, I., Brooke, T.Y., Hartmann, L., & Calvet, N. 2009, *ApJ*, 702, 1507  
 Morris, D.H., Mutel, R.L., & Su, B. 1990, *ApJ*, 362, 299  
 Papaloizou, J. C. B., & Nelson, R. P. 2005, *A&A*, 433, 247  
 Papaloizou, J.C.B., Nelson, R.P., Kley, W., Masset, F.S., & Artymowicz, P. 2007, *Protostars and Planets V*, 655  
 Quillen, A.C., & Trilling, D.E. 1998, *ApJ*, 508, 707  
 Rafikov, R.R. 2002, *ApJ*, 572, 566  
 Ray, T., Dougados, C., Bacciotti, F., Eisloffel, J., & Chrysostomou, A. 2007, in *Protostars and Planets V*, B. Reipurth, D. Jewitt, & K. Keil (eds.), University of Arizona Press, Tucson, p. 231  
 Romanova, M.M., & Kulkarni, A.K. 2009, *MNRAS*, 398, 1105  
 Romanova, M.M., Ustyugova, G.V., Koldoba, A.V., & Lovelace, R.V.E. 2002, *ApJ*, 578, 420  
 Romanova, M.M., Ustyugova, G.V., Koldoba, A.V., & Lovelace, R.V.E. 2004, *ApJ*, 610, 920  
 Romanova, M.M., & Kulkarni, A.K. 2009, *MNRAS*, 398, 1105  
 Romanova, M.M., Ustyugova, G.V., Koldoba, A.V., & Lovelace, R.V.E. 2009, *MNRAS*, in press (*arXiv:0907.3394*)  
 Sánchez-Lavega, A. 2004, *ApJ*, 609, L87  
 Skinner, S.L., & Brown, A. 1994, *AJ*, 107, 1461  
 Triaud, A.H.M.J., Cameron, A.C., Queloz, D., Anderson, D.R., Gillon, M., Hebb, L., Hellier, C., Loeillet, B., Maxted, P.F.L., Mayor, M., Pepe, F., Pollacco, D., Ségransan, D., Smalley, B., Udry, S., West, R.G., & Wheatley, P.J. 2010, *A&A*, submitted  
 Warner, B. 2004, *PASP*, 116, 115